Electron transfer in dextran probed by longitudinal field muon spin relaxation

2007 J. Phys.: Condens. Matter 19 026221

(http://iopscience.iop.org/0953-8984/19/2/026221)

INSTITUTE OF PHYSICS PUBLISHING JOURNAL OF PHYSICS: CONDENSED MATTER

J. Phys.: Condens. Matter **19** (2007) 026221 (9pp) doi:10.1088/0953-8984/19/2/026221

Electron transfer in dextran probed by longitudinal field muon spin relaxation

M T F Telling[1,3] **and S H Kilcoyne**[2]

[1] ISIS Facility, Rutherford Appleton Laboratory, Chilton, OX11 0QX, UK
[2] Institute for Materials Research, University of Salford, Salford M5 4WT, UK

E-mail: M.Telling@rl.ac.uk and S.H.Kilcoyne@salford.ac.uk

Received 2 October 2006, in final form 18 November 2006
Published 15 December 2006
Online at stacks.iop.org/JPhysCM/19/026221

Abstract

Electron-transfer processes play a crucial role in bio-nanobattery design, the electron transfer rate through the organic material being a key parameter in determining the resistance, maximum current, power density, discharge rate and duty cycle of the cell. The labelled electron method using positive muons allows such transfer processes in macromolecules, such as polymers and proteins, to be probed on a microscopic level. Here we present the results of an experiment using the labelled electron method with longitudinal field muon spin relaxation (LF-μSR) to investigate electron-transfer processes in dextran. The data are well described using the Risch–Kehr model and the results suggest intra-chain diffusion is the dominant transport process in this system between 15 and 250 K. Intra-chain diffusion rates of 10^{13} s^{-1} have been determined.

1. Introduction

As the size of electrical circuits and components is reduced, the need for a miniaturized distributed power system with negligible Joule heating increases. One possible route to satisfy this demand is the development of bio-nanobatteries: lightweight, high energy density, nanometre-scale electrical energy storage devices based upon organic material. Due to their size, bio-nanobatteries have the potential to be incorporated into numerous devices, including ultra-high density data storage media [1], nano-electromagnetic systems [2], quantum electronic devices [3] and biochips. Work has already been carried out in the US to develop bio-nanobatteries based upon the iron storage protein ferritin.

Ferritin is the normal iron storage protein found in all living things including plants, bacteria and animals. A ferritin molecule is composed of an iron-based core of up to 4500 Fe (III) ions in a ferrihydrite-like composition, attached by covalent bonding to carboxylate residues inside a spherical protein shell of internal diameter ∼8 nm. This protein shell, which is ∼2 nm thick and referred to as apoferritin, is composed of 24 polypeptide chains which

[3] Author to whom any correspondence should be addressed.

span the edges of a rhombic dodecahedron as anti-parallel pairs. Ferritin is therefore an almost spherical molecule ∼12 nm in diameter. The use of ferritin as a nano-battery has two distinct advantages. First, the material can be reconstituted with a variety of metallic cores (e.g. Fe, Co, Ni, or Pt), each with a different redox capability, which offers the possibility of optimizing the properties of the battery by modifying the core. Second, a ferritin-based nanobattery is likely to be biocompatible, increasing its potential to include applications in medicine.

King *et al* [4] at NASA are currently working on a project to develop a bio-nanobattery based upon multi-layer arrays of reconstituted ferritin, and they have already developed a five-cell demonstrator based on Fe- and Co-reconstituted ferritins for proof of concept and characterization. Indeed, King *et al* have measured an electrical output of nearly 0.5 V for the battery cell. Despite the initial success of King *et al*'s research several challenges still remain, such as increasing the energy density, before such a battery can become a commercially viable concept. While King *et al* propose to address these problems by manipulating the ferritin core itself, it should also be possible to enhance the properties of this prototype battery by optimizing the surrounding organic material. It is this hypothesis which has stimulated the work presented here.

Electron-transfer processes play a crucial role in bio-nanobattery design, the electron transfer rate through the organic material being a key parameter in determining the resistance, maximum current, power density, discharge rate and duty cycle of the cell. In addition to the conventional laboratory-based methods which exist for measuring conductivity, it has recently been shown that through a combination of longitudinal field muon spin relaxation (LF-μSR) measurements and a theoretical framework developed by Risch and Kehr [5] it is possible to determine electron diffusion rates in conducting polymers [6] and macromolecules such as proteins [7] and DNA [8]. μSR [9] is a microscopic probe which measures the time-dependent spin dynamics of an excitation from which the transport properties can be determined. It has an advantage over other techniques, such as ESR and NMR, since it can both generate an excitation and then act as a probe of the dynamical properties of the excitation. We have already used the labelled electron method using positive muons to characterize electron transfer in the protein apoferritin, the Fe-depleted form of ferritin [10], and in this paper have extended our work to investigate electron transfer in the Fe-depleted form of iron–dextran, a pharmaceutical equivalent to ferritin used in the treatment of iron deficiency anaemias. Iron–dextran is similar to ferritin in that it consists of an Fe-based core approximately 6 nm in diameter surrounded by an organic shell of dextran, a polymer of anhydroglucose $(C_6H_{10}O_5)_n$ having mainly α-D-(1 $\rightarrow$ 6) linkages with some unusual 1,3-glucosodic linkages at branching points [11]. This shell can be between 2 and 15 nm thick [12].

If the electron-transfer processes in dextran are comparable to those observed in the apoferritin it is conceivable that bio-nanobatteries can be constructed from Fe–dextran complexes. Like ferritin, Fe–dextrans are biocompatible but have the additional advantage that they can be manufactured with a range of shell thickness which may allow the electron-transfer rates to be tailored for specific needs. To the best of our knowledge electron transfer has not been studied in dextran, and therefore in this paper we present the results of the first study of electron transfer in dextran using the labelled electron method with positive muons.

2. Longitudinal field muon spin relaxation (LF-μSR)

When positive muons, μ^+, are deposited in a chemical sample at least three possible events can occur:

(i) μ^+ sits in the sample and decays with its characteristic lifetime of 2.2 μs, emitting a positron preferentially in the direction of the muon spin according to the expression,

$W_o = 1 + a_o \cos\theta$, where θ is the angle between the muon spin and the direction of positron emission.

(ii) μ^+ combines with an electron to form a muonium atom, Mu, a radioactive light isotope of hydrogen.

(iii) Mu reacts with the substrate to form a muonium-substituted radical, or resides in a diamagnetic environment.

All of these events can be detected and characterized using either the (zero-field) ZF-μSR or LF-μSR technique. Previous work by Kilcoyne and Webster [11] has shown that when muons are implanted into dextran they either reside at sites within the material or form muonium. When muonium atoms are formed, as in (ii), 50% of the polarization is lost. Full spin polarization can be recovered by the application of a magnetic field along the direction of the spin polarization, the muon and electron spins being decoupled by the applied magnetic environment.

3. Modelling muon relaxation spectra

As both LF- and ZF-μSR are well established and described in detail elsewhere [9], only a summary is given here. In both ZF- and LF-μSR experiments, detectors are positioned along the beam direction in front of, and behind, the sample. Relaxation spectra are determined from the time-dependent positron count rates in the forward $F(t)$ and backward $B(t)$ detectors via the expression

$$P(t) = a_o G_z(t) = \frac{F(t) - \alpha B(t)}{F(t) + \alpha B(t)} \tag{1}$$

where $P(t)$ is the time dependent muon spin polarization, a_o is the initial asymmetry at time $t = 0$ and α is a calibration term to account for the relative efficiencies of the forward and backward detectors and for absorption within the sample and the cryostat. α is determined from the room-temperature spectrum collected in a small transverse magnetic field of 2 mT. $G_z(t)$ is the longitudinal muon spin relaxation function.

Risch and Kehr (RK) [5] considered the spin relaxation of a muon interacting with an electronic spin defect that is rapidly diffusing along a one-dimensional (1D) chain in both zero, and applied, magnetic field. For finite fields, RK predict that depolarization of the muon spin can be modelled using a relaxation function of the form

$$G_z(t) = \exp(\Gamma(B)t)\mathrm{erfc}((\Gamma(B)t)^{1/2}). \tag{2}$$

Here, erfc signifies the complementary error function and $\Gamma(B)$ is a magnetic field-dependent RK relaxation parameter. Satisfactory description of experimental data using (2) suggests that the mean time between electronic defect spin flips, λ, is short compared to the experimental timescale, $t_{\max}$. The relaxation function follows a $t^{-1/2}$ form [13] at long times rather than showing an exponential decay as observed in early μSR studies of conducting polymers [14]. It should be mentioned that while Risch and Kehr considered spin relaxation in zero applied field, application of their model function to experimental zero-field data from *trans*-polyacetylene proved unsatisfactory. It has been suggested that the reduced quality of fit observed in zero field is because the RK model neglects dipolar coupling of the muon to the surrounding protons. Such interaction becomes decoupled by the application of fields of the order 10 G or larger. In finite magnetic fields, B, however, the RK relaxation parameter, $\Gamma(B)$ is given by

$$\Gamma(B) = \lambda/(1 + (2\omega_e\lambda)^{1/2} D_\parallel/\omega_o^2)^2 \tag{3}$$

where $\omega_e = \gamma_e B$ (γ_e is the gyro-magnetic ratio of the electron and equal to 1.76×10^{11} Hz T^{-1}), ω_o ($=2\pi A$) is the muon–electron hyperfine coupling frequency and $D_\parallel$ is the intra-chain,

or 1D, diffusion rate. ω_o is obtained from the longitudinal decoupling field, B_o, of the initial muon asymmetry. B_o is determined from polarization curves via the expression $P = 1/2(1 + (x^2/1 + x^2))$ where $x = B/B_o$ and $B_o = A_\mu/(\gamma_\mu + \gamma_\varepsilon)$. A_μ is the hyperfine coupling between the muon and electron, which is assumed to be isotropic, and γ_μ and γ_e are muon and electron gyro-magnetic ratios respectively. It is usual to cite muon–electron hyperfine coupling constants, A_μ, in a reduced form $A'_\mu = A_\mu\ (\mu_p/\mu_\mu) = 0.3141 A_\mu$, where μ_p is the magnetic moment of a proton and μ_μ is the muon magnetic moment. Kilcoyne and Webster [11] showed A'_μ ($=A_\mu \times 0.3141$) to be approximately constant in dextran over the temperature range 15–250 K with a mean value of 897 ± 22 MHz. Consequently, $A_\mu = 2856 \pm 70$ MHz. In the fast intra-chain diffusion limit, $\Gamma(B)$ is predicted to exhibit a B^{-1} inverse magnetic field dependence and the intra-chain diffusion rate, $D_\parallel$, can be determined from the expression,

$$D_\parallel^2 = \omega_o^4/2\omega_e\Gamma(B). \tag{4}$$

As the field is reduced, however, a cut off in the inverse field dependence may be observed such that $\Gamma(B)$ becomes approximately field independent. The critical field at which this cut off occurs is the field at which ω_e becomes smaller than the inter-chain, or 3D, diffusion rate, $D_\perp$. Should such a response be observed then an estimate of the inter-chain diffusion rate, $D_\perp$, can be obtained by assuming that the field-dependent behaviour of Γ has the form

$$\Gamma(B) = \Gamma_o/(1 + (B/B_c)) \tag{5}$$

where B_c is the critical field above which $\Gamma(B)$ evolves from field independent to field dependent. $D_\perp$ can be determined using $D_\perp = \gamma_e B_c$. The RK model of spin relaxation has been applied successfully to several systems, for example, in μSR studies of electron motion in the conducting and non-conducting polymers, polyaniline and polypyridine [6], and in proteins such as cytochrome-c, myoglobin [7] as well as DNA [8]. The RK form has also been used to successfully described muon spin depolarization in apoferritin [10], the results of which are compared and contrasted to dextran in this paper.

4. Experimental details

Muon spin relaxation measurements were conducted on the EMU spectrometer at the ISIS Muon Facility, Rutherford Appleton Laboratory, UK [15]. Approximately 2 g of dextran from *Leuconostoc mesenteroides*, Strain No. B-512 (Sigma Chemicals, UK) was wrapped in thin silver foil and mounted in a helium cryostat. Spectra were collected over a time range of 0.1–16 μs in zero field and in applied longitudinal magnetic fields between 80 and 3800 G (8 and 380 mT) for a selection of temperatures between 15 and 250 K. Room-temperature data were also collected both for a pure (99.99%) silver sample and a quartz plate as a function of applied longitudinal field for calibration purposes. Relaxation spectra $G_z(t)$ were determined from the forward, $F(t)$, and backward, $B(t)$, time-dependent positron count rates using equation (1) and a calibration factor of $\alpha = 0.88$.

5. Results and discussion

Examples of the μSR relaxation spectra determined from the forward $F(t)$ and backward $B(t)$ time-dependent positron count rates are shown in figure 1. Data collected at finite field are well described by the RK model. However, the quality of fit of the RK model to the experimental zero-field data is unsatisfactory. As previously mentioned, this reduced quality of fit observed at zero field is most likely due to the fact that the RK model neglects dipolar coupling of the muon to the surrounding protons. Such interaction becomes decoupled by the application of

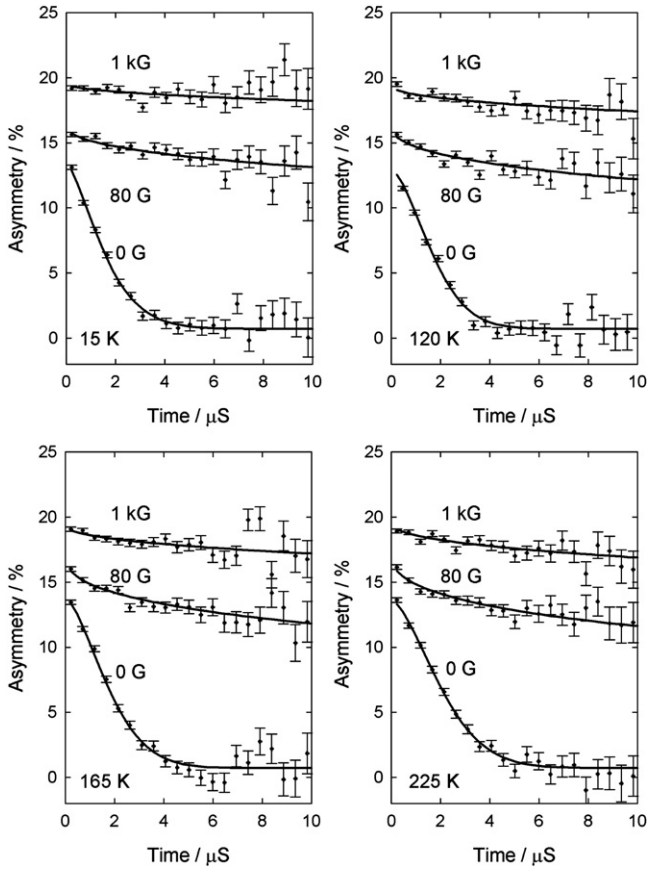

Figure 1. Typical μSR spectra collected at 15, 120, 165 and 225 K and at the applied fields indicated. The solid lines are fits to the data using the functions described in the text.

fields of the order 10 G or larger. Instead, we find that the zero-field spectrum is best modelled using a phenomenological stretched exponential function of the form $P(t) = a_o \exp(-\lambda t)^{\beta}$. Here a_o is the muon asymmetry at time $t = 0$, and the exponent β shows no temperature dependence, within error, between 15 K ($\beta = 1.44 \pm 0.06$) and 250 K ($\beta = 1.47 \pm 0.06$). In both models it is necessary to include a temperature- and time-independent term, a_{bck}, to account for those muons which thermalize in the silver mask surrounding the sample. The magnitude of a_{bck} was obtained by fitting the lowest temperature (15 K) zero-field data to $P(t) = a_o \exp(-\lambda t)^{\beta} + a_{\mathrm{bck}}$. The resulting background value, $a_{\mathrm{bck}} = 0.712\%$, was fixed while fitting all subsequent temperatures and fields.

Following the analysis procedure previously outlined, a value of the RK relaxation parameter, Γ, was obtained for each measured temperature and for fields of 80 G and above. The field dependence of Γ at 15, 120, 165 and 225 K is shown in figure 2.

At high fields ($B_{\mathrm{ext}} > 500$ G), the relaxation parameter, Γ, is inversely proportional to B_{ext} over the entire temperature range studied. Risch and Kehr predict that at low fields there may be a cut off in the observed inverse-field behaviour such that $\Gamma(B)$ becomes approximately field independent. The critical field at which this cut off occurs is the field at which ω_{e} becomes smaller than the inter-chain, or 3D, diffusion rate. No such field-independent region is observed

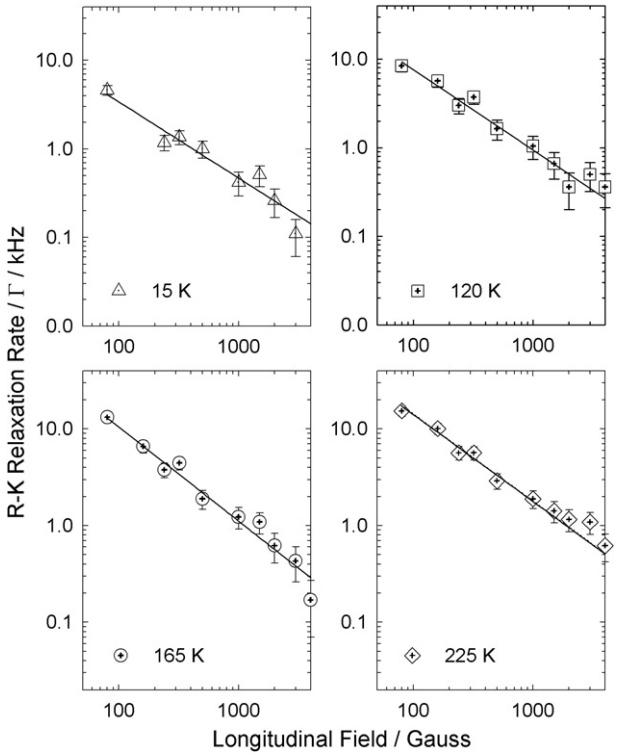

Figure 2. The field dependence of the RK relaxation parameter, Γ, at 15, 120, 165 and 225 K. The solid lines are the result of fitting: $\Gamma(B) = \text{Constant} \times B^{-\gamma}$. The critical exponents, γ, for each fit (in ascending temperature) are 1.1 ± 0.1, 0.91 ± 0.09, 0.88 ± 0.06 and 0.9 ± 0.1 respectively. $\Gamma(B)$ is seen to approximate to a B^{-1} dependence.

in the dextran data. Instead Γ remains inversely proportional to applied field between 80 and 4000 G. Indeed, for each measured temperature $\Gamma(B)$ is well described using a power law, $\Gamma(B) = C \times B^{-\gamma}$, where C is a constant of proportionality. The critical exponent, γ, is found to be close to unity, within error, between 15 and 250 K, illustrating that $\Gamma(B)$ approximates to a B^{-1} form. Such inverse field dependence is predicted by Risch and Kehr to be indicative of intra-chain, or 1D, diffusion. Our results therefore suggest that 1D diffusion is the dominant transport process in dextran over the temperature range 15 K $<$ T $<$ 250 K. In addition, the satisfactory description of the muon spin depolarization in dextran using the RK model (2) suggests that between 15 and 250 K the mean electronic spin flip rate is short compared to the experimental timescale.

The equivalent $\Gamma(B, T)$ data obtained from apoferritin shows a similar linear response between 15 K $< T <$ 270 K and for applied fields between 50 and 3800 G [10]. However, in contrast to dextran, an inflexion is observed at approximately 800 G in the protein $\Gamma(B, T)$ data, the point of inflexion showing no pronounced temperature dependence. There is no obvious inflexion in any of the dextran data.

The evolution of Γ as a function of temperature, and with the dextran sample subjected to an applied field of 1 kG, is shown in figure 3. The response of Γ (1 kG, T) from apoferritin is also shown for comparison (figure 3 (inset)). It should be noted that we do not expect an applied field of 1 kG to have any particular significance but have chosen to analyse the temperature

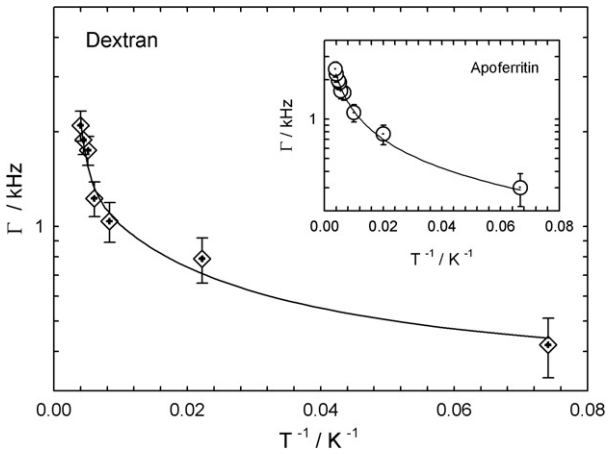

Figure 3. Temperature dependence of the RK relaxation rate from dextran in an applied field of 1 kG. Inset: evolution of Γ (1 kG, T) from apoferritin. The solid lines are a guide to the eye.

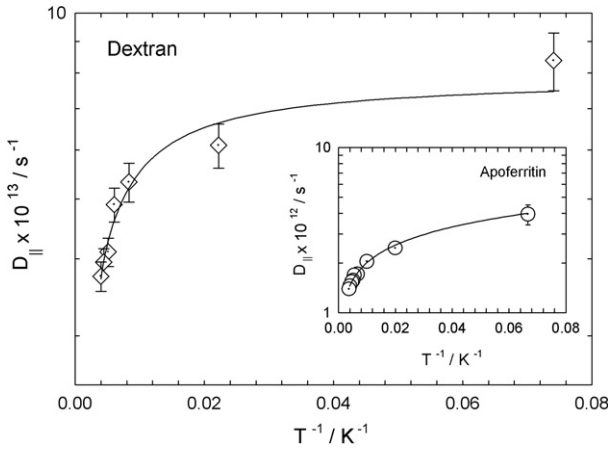

Figure 4. Temperature dependence of the intra-chain diffusion rate at 1 kG from dextran derived from (4). Inset: temperature dependence of the intra-chain diffusion rate at 1 kG from apoferritin [10]. The solid lines are guides to the eye.

dependence of Γ (1 kG) in more detail to allow comparisons to be drawn between this work and that reported by other authors [6–8]. Γ rises from 0.42 kHz at 15 K to 2.1 kHz by 250 K. The magnitude and thermal response of Γ (1 kG) in dextran is comparable to that observed in apoferritin.

The corresponding intra-chain diffusion rate, $D_{\|}$, shown in figure 4 was determined by fitting the high-field Γ (1 kG) data to (4). Again, $D_{\|}$ (1 kG, T) from apoferritin is shown alongside for comparison (figure 4 (inset)). For dextran, diffusion rates of the order 10^{13} s^{-1} are obtained at all temperatures. In order to derive $D_{\|}$ (1 kG, T) a muon–electron hyperfine coupling frequency of $\omega_o = 2\pi A$ was assumed, where A (=2856 MHz ± 70 MHz) is the muon–electron hyperfine coupling constant determined from muonium repolarization measurements [11]. A is reported to be temperature independent, within error, between 13 and 250 K. $D_{\|}$ (1 kG, T) is seen to decrease non-linearly with increasing temperature.

Again, the temperature dependence and magnitude of $D_{\|}(T)$ is comparable to that determined for apoferritin. However, while dextran exhibits intra-chain diffusion rates, $D_{\|}$ (1 kG, T), of the order 10^{13} s^{-1}, $D_{\|}$ calculated for apoferritin is a order of magnitude lower at 10^{12} s^{-1}. $D_{\|}(T)$ for dextran is also one to two orders of magnitude larger than the mean values reported for the proteins, myoglobin ($\sim 10^{11}$ s^{-1}) and cytochrome-c ($\sim 10^{12}$ s^{-1}) [7] and for the conducting polymers, polyaniline and polypyridine (both $\sim 10^{11}$ s^{-1}) [6]. Nevertheless, the form of $D_{\|}(T)$ observed from all five materials is comparable, with $D_{\|}(T)$ decreasing as the temperature is elevated. For polyaniline and polypyridine the decrease in $D_{\|}(T)$ at high temperatures is reportedly suggestive of phonon-limited metallic-like transport, where $D_{\|}(T)$ is modelled using a simple optical-phonon-limited transport equation [6].

As previously mentioned, when ω_e becomes smaller than the inter-chain, or 3D, diffusion rate there will be a cut off in the inverse field dependence and $\Gamma(B)$ will become approximately field independent. No such field-independent region is observed in the dextran data; instead, Γ remains inversely proportional to applied field from 80 to 4000 G at all temperatures, suggesting that intra-chain diffusion occurs over the whole temperature range. While this is comparable to the results obtained from apoferritin, myoglobin and cytochrome-c exhibit both inter- and intra-diffusion characteristics. It is interesting to note that while the samples of myoglobin and cytochrome-c both contain Fe, apoferritin and dextran do not. It is therefore possible that the change in the field dependence of Γ observed in myoglobin and cytochrome-c, and interpreted by the authors as an evolution from inter- to intra-chain diffusion, in reality arises in part from the muon or electronic spin defect sensing the magnetic moment of the Fe atoms. It is also interesting to note that the RK model provides an excellent description of the data despite the fact that dextran consists of a loosely coiled chain of pyranose rings rather than a 1D linear chain conformation as modelled by Risch and Kehr in their original paper.

6. Conclusions

We have used the labelled electron method via longitudinal field muon spin relaxation (μSR) to characterize electron-transfer processes in the anhydroglucose polymer, dextran, with a view to the future development of bio-nanobatteries. Data collected at finite fields ($B_{\text{ext}} \geqslant 80$ G) are well described using the Risch–Kehr model at all measured temperatures.

Between 80 and 4000 G, and over the temperature range studied here (15 K $\leqslant$ T $\leqslant$ 250 K), the RK relaxation parameter, Γ, is inversely proportional to the applied field, B_{ext}. Moreover, the form of $\Gamma(B)$ approximates to a B^{-1} dependence. Such behaviour is predicted by Risch and Kehr to be indicative of intra-chain, or 1D, diffusion. None of the characteristics of inter-chain, or 3D, diffusion are observed. With the dextran sample subject to an applied field of 1 kG, $\Gamma(T)$ is seen to rise as the temperature is elevated, the magnitude and temperature dependence of $\Gamma(T)$ being comparable to that observed in apoferritin. In addition, the temperature dependence of the intra-chain diffusion rate, $D_{\|}$, at 1 kG for dextran is comparable to that observed in the proteins myoglobin and cytochrome-c, as well as the conducting polymers polyaniline and polypyridine. However, at 10^{13} s^{-1} the magnitude of $D_{\|}$ in dextran is at least an order of magnitude larger that the values reported for these other systems. This large diffusion rate suggests that electron transfer in dextran is rapid, and we therefore believe that the applicability of dextrans for the future development of bio-nanobatteries should be explored further.

Acknowledgments

The authors would like to thank the UK's Engineering and Physical Sciences Research Council for access to the ISIS facility, Rutherford Appleton Laboratory and Drs Judith Gretton-Dann,

Francis Pratt, Philip King and Stephen Cottrell for assistance with the muon experiments and fruitful discussions.

References

[1] Warne B, Kasyutich O I, Mayes E L, Wiggins J A L and Wong K K W 2000 *IEEE Trans. Magn.* **36** 3009
[2] Kahn O 1993 *Molecular Magnetism* (New York: VCH)
[3] 1999 *Nano Struct. Sci. Technol.*
[4] http://techreports.larc.nasa.gov/ltrs/PDF/2004/mtg/NASA-2004-11isssm-gck.pdf
[5] Risch R and Kehr K W 1992 *Phys. Rev.* B **46** 5246–57
[6] Pratt F L, Blundell S J, Jestadt Th, Lovett B W, Husmann A, Marshall I M, Hayes W, Monkman A P, Watanabe I, Nagamine K, Martin R E and Holmes A B 2000 *Physica* B **625** 289–90
[7] Nagamine K, Pratt F L, Ohira S, Watanabe I, Ishida K, Nakamura S N and Matsuzaki T 2000 *Physica* B **289/290** 631–5
[8] Nagamine K and Torikai E 2004 *J. Phys.: Condens. Matter* **16** S4797–806
[9] Brewer J H and Cywinski R 1999 *Muon Science: Muons in Physics, Chemistry, and Materials* ed S L Lee, S H Kilcoyne and R Cywinski (London: IoP Publishing) chapter 1
[10] Telling M T F and Kilcoyne S H 2006 *Physica* B **374–375** 451–5
[11] Kilcoyne S H and Webster B 2000 *Magn. Reson. Chem.* **38** S20–6
[12] Cox E M, Bereman R D and Monte W T 1995 *J. Inorg. Biochem.* **60** 149–53
[13] Pratt F L 2004 *J. Phys.: Condens. Matter* **16** S4779–96
[14] Nagamine K and Ishida K 1986 *Hyperfine Interact.* **32** 535–49
[15] Eaton G H, Clarke-Gayther M A, Scott C A, Uden C N and Williams W G 1994 *Nucl. Instrum. Methods* A **342** 319–31